Journal of Quantitative Spectroscopy & Radiative Transfer 258 (2021) 107352

Contents lists available at ScienceDirect

Journal of Quantitative Spectroscopy & Radiative Transfer

journal homepage: www.elsevier.com/locate/jqsrt

Line lists for the $X^2\Sigma^+$-$X^2\Sigma^+$, $A^2\Pi$-$A^2\Pi$ and $A^2\Pi$-$X^2\Sigma^+$ transitions of CP

Zhi Qin[a,b], Tianrui Bai[b,c], Linhua Liu[b,c,*]

[a] School of information science and Engineering, Shandong University, Qingdao 266237, China
[b] Optics and Thermal Radiation Research Center, Shandong University, Qingdao 266237, China
[c] School of Energy and Power Engineering, Shandong University, Jinan 250061, China

ARTICLE INFO

Article history:
Received 4 August 2020
Revised 20 September 2020
Accepted 22 September 2020
Available online 25 September 2020

Keywords:
MARVEL energy levels
Electronic structures
Analytical spectroscopic models
Carbon monophosphide

ABSTRACT

Rovibrational energy levels of CP are investigated for its $X^2\Sigma^+$ and $A^2\Pi$ electronic states. Rovibronic frequencies observed experimentally for the $A^2\Pi$-$X^2\Sigma^+$ transition are used to produce empirical energy levels with the MARVEL method (denoted as MARVEL energy levels). The MARVEL energy levels for the $X^2\Sigma^+$ and $A^2\Pi$ states are then employed to fit the empirical potential energy curves (PECs), spin orbit coupling curves (SOCCs) and electronic angular momentum curves (EAMCs) by using the DUO program, also constrained by the corresponding *ab initio* curves. Meanwhile, empirical Born-Oppenheimer breakdown curves, spin-rotation curves (SRCs), Λ-doubling curves are also added to well reproduce the MARVEL energy levels. These curves referred to as analytical spectroscopic models are as an input to DUO to obtain the fitted energy levels for the $X^2\Sigma^+$ and $A^2\Pi$ states and the line lists for the $X^2\Sigma^+$-$X^2\Sigma^+$, $A^2\Pi$-$A^2\Pi$ and $A^2\Pi$-$X^2\Sigma^+$ transitions. Partition functions for temperatures up to 5000 K are computed by using the fitted energy levels and fitted by polynomial expansions. The calculated MARVEL energies can be used for spectroscopic investigations of the interstellar CP radical in various astrophysical sources, especially in circumstellar envelopes and warm clouds. The rovibrational energy levels and line lists derived from the analytical spectroscopic models can be used for predicting spectroscopy at temperatures up to 5000 K for potential applications in related plasmas.

1. Introduction

Over the past ten years or so, several P-containing molecules, such as PN, PO, CP, HCP and PH_3, have been discovered in a variety of astrophysical sources [1-16]. Observations show that the chemistry of phosphorus seems active in carbon-rich envelopes of evolved stars. Astronomers infer that carbon monophosphide (CP) is likely to be the photodissociation product at larger radii of the carbon star IRC+10,216 [4,16]. Spectroscopic information of CP could be helpful for searching for the interstellar CP and better understanding of phosphorus chemistry in space [17].

There have been several studies that aimed at achieving energy levels and line frequencies of CP from experimental measurements and *ab initio* calculations [18-36]. A summary of previous experimental and theoretical studies of CP is given by Shi et al. [33]. Similar summaries are also provided by Abbiche et al. [34] and Qin et al. [36]. Early observations of two doublet electronic transition systems ($B^2\Sigma^+$-$X^2\Sigma^+$ and $B^2\Sigma^+$-$A^2\Pi$) obtained a set of spectroscopic parameters of the $X^2\Sigma^+$, $A^2\Pi$ and $B^2\Sigma^+$ electronic states for CP [18,19,23]. Subsequently, Ram et al. [24,27] observed a high-resolution spectra of the $A^2\Pi$-$X^2\Sigma^+$ system for CP using a Fourier transform infrared spectrometer and the transition frequencies of the bands involving vibrational levels up to υ =4 for both the $X^2\Sigma^+$ and $A^2\Pi$ electronic states are available.

Ab initio calculations of CP prior to 2014 focused mainly on the potential energy curves (PECs) and spectroscopic parameters of its low-lying electronic states [29-31,33,34]. Various *ab initio* methods and basis sets were considered to improve the accuracy of the PECs. Abbiche et al. [34] also calculated the diagonal $<A^2\Pi|H^{SO}|A^2\Pi>$ and off-diagonal $< X^2\Sigma^+|H^{SO}|A^2\Pi>$ spin-orbit coupling (SOC) integrals for the internuclear distance R = 2.5–6.5 bohr. Our recent *ab initio* study of CP, also relevant to the present work, has been published with detail calculations of PECs for sixteen low-lying electronic states using the icMRCI+Q/56+CV+DK method, as well as of the transition dipole moment curves (TDMCs) for nineteen dipole-allowed transitions at the icMRCI/AV6Z level of theory [36].

Limited work has been carried out on producing line lists of CP. The Cologne Database for Molecular Spectroscopy (CDMS) database

* Corresponding author.
E-mail address: liulinhua@sdu.edu.cn (L. Liu).

https://doi.org/10.1016/j.jqsrt.2020.107352
0022-4073/

contains 345 hyperfine transitions associated with the υ =0 vibrational level of the $X^2\Sigma^+$ electronic ground state [37]. A more elaborate line list for CP was given by Ram et al. [35], who presented a list of transition wavenumbers and intensities of the $A^2\Pi$-$X^2\Sigma^+$ system with υ =0–8 for both $X^2\Sigma^+$ and $A^2\Pi$ electronic states using Rydberg-Klein-Rees (RKR) potentials and *ab initio* electronic TDM.

This paper aims to present rovibrational energy levels of the $X^2\Sigma^+$ and $A^2\Pi$ electronic states and the line lists of the $X^2\Sigma^+$-$X^2\Sigma^+$, $A^2\Pi$-$A^2\Pi$ and $A^2\Pi$-$X^2\Sigma^+$ transitions for CP. The empirical energy levels are generated by the MARVEL method based on available experimental wavenumbers of the $A^2\Pi$-$X^2\Sigma^+$ system. The empirical PECs are fitted by the MARVEL energy levels and also constrained by *ab initio* ones. To well produce the MARVEL energy levels, the spin-orbit coupling curves (SOCCs), electronic angular momentum curves (EAMs), Born-Oppenheimer breakdown curves, spin-rotation curves (SRCs), Λ-doubling curves are also considered. Finally, these curves are added to nuclei motion equation of diatomic molecules which can be accomplished by DUO program to generate the rovibrational energy levels of the $X^2\Sigma^+$ and $A^2\Pi$ states and the line lists of the $X^2\Sigma^+$-$X^2\Sigma^+$, $A^2\Pi$-$A^2\Pi$ and $A^2\Pi$-$X^2\Sigma^+$ transitions for CP. The fitted rovibrational energy levels are then used to compute the partition functions for temperatures up to 5000 K. Finally, our line lists are used to simulate spectra and compare with available experimental ones.

2. The MARVEL methodology

MARVEL (Measured Active Vibration Rotation Energy Levels) is a well established algorithm [38-41] based on the theory of spectroscopic networks [42-45] and can invert high-resolution experimental wavenumbers (or frequencies) to accurate empirical energy levels and associated uncertainties. The latest version [41] has led to greatly improved treatment of uncertainties and hence can generate high quality data. The MARVEL method has been applied to many diatomic molecules, including $^{48}Ti^{16}O$ [46], $^{90}Zr^{16}O$ [47], $^{16}O_2$ [48], ^{14}NH [49], etc.

Experimentally, the high-resolution rotationally-resolved wavenumbers of the $A^2\Pi$-$X^2\Sigma^+$ transition were investigated by Ram et al. [24,27,35]. According to the main text of Ram et al. [35], the $A^2\Pi_{1/2}$ is about 156 cm^{-1} higher than the $A^2\Pi_{3/2}$ component. However, the assignment of the $A^2\Pi_{1/2}$ energy and the $A^2\Pi_{3/2}$ energy in the supplemental material of Ram et al. [35] seems to be exchanged each other. By critically evaluation of the results of Ram et al. [35] and the *ab initio* energies from Abbiche et al. [34], we suspect the supplemental material of Ram et al. [35] includes the typo of an energy exchange between the $A^2\Pi_{1/2}$ component and the $A^2\Pi_{3/2}$ component. Finally, the experimental transition wavenumbers of the $A^2\Pi$-$X^2\Sigma^+$ transition with an uncertainty of 0.001 cm^{-1} were chosen as an input to the MARVEL algorithm. A set of 353 empirical rovibrational energy levels of the $X^2\Sigma^+$ state and 595 empirical rovibrational energy levels of the $A^2\Pi$ state was then generated. The observed 3264 rovibronic wavenumbers for the $A^2\Pi$-$X^2\Sigma^+$ system span the (0,0), (0,1), (0,2), (1,0), (1,3), (2,0), (2,2), (2,4), (3,1), (3,3) and (4,3) bands with rotational coverage up to a maximum $J = 46.5$. The produced each MARVEL energy level with a unique and self-consistent set of quantum numbers and an appropriate uncertainty is given in the supplemental Material.

Comparisons of the empirical energy levels from Ram et al. [35] (denoted as $E_{14RaBrWeBe}$) with MARVEL data are displayed in Fig. 1 for the $X^2\Sigma^+$ state and in Fig. 2 for the $A^2\Pi$ state. In Fig. 1, the residuals $E_{14RaBrWeBe}$-E_{MARVEL} for the $X^2\Sigma^+$ state energies are plotted versus the rotational quantum number J for υ up to 4. In Fig. 2, the residuals $E_{14RaBrWeBe}$-E_{MARVEL} for the $A^2\Pi$ state energies are plotted versus the rotational quantum number J for υ up to 4.

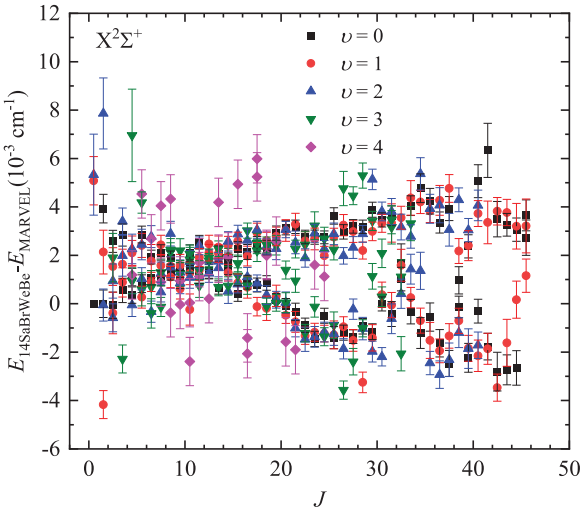

Fig. 1. Comparison of the empirical energy levels for the $X^2\Sigma^+$ state from Ram et al. [35] with the MARVEL data. The residuals $E_{14RaBrWeBe}$-E_{MARVEL} for energy term values are plotted versus the rotational quantum number J for υ up to 4. The vertical bars represent the values of the uncertainty for MARVEL energy term values.

The vertical bars in Fig. 1 and Fig. 2 are expressed as the uncertainty of the MARVEL energy term values. As shown in Fig. 1, the agreement of the empirical energy levels from Ram et al. [35] with the MARVEL energy term values is within the uncertainty from 0.07×10^{-3} cm^{-1} to 6×10^{-3} cm^{-1} for the $X^2\Sigma^+$ state. For the $A^2\Pi$ state in Fig. 2, the coincidence of most energy levels from Ram et al. [35] with the MARVEL data is within the uncertainty of 5×10^{-3} cm^{-1}.

3. DUO and spectroscopic models

DUO is a general program that is developed by ExoMol group in University College London [50] and can compute rotational, rovibrational and rovibronic spectra of diatomic molecules [51]. Its main features include fitting the analytical potential energy functions and other coupling curves constrained by possible *ab initio* ones to the experimental energy term values or wavenumbers and solving the Schrödinger equation for the motion of the nuclei with the consideration of an arbitrary number and type of couplings between electronic states. DUO has been successfully applied to generate spectroscopic data of many diatomic molecules, including CaO [52], MgO [53], AlH [54], C_2 [55], PO and PS [56], etc.

The aim of this section is to fit analytical potential energy functions and other coupling curves to the experimental energy term values and generate the line lists for CP. For avoiding the unphysical behavior of the fitted analytical functions, the *ab initio* electronic structure curves are needed. So completing such a fit includes two steps: (a) Solving the electronic Schrödinger equation in order to obtain the PECs, SOCCs and EAMCs; (b) Improving *ab initio* PECs, SOCCs and EAMCs by fitting experimental energy terms to obtain analytical curves. During the fitting, empirical Born-Oppenheimer breakdown curves, SRCs and Λ-doubling curves are also added to well reproduce the experimental energy term values.

3.1. Electronic structure computations

Ab initio PECs of the $X^2\Sigma^+$ and $A^2\Pi$ electronic states are computed using the complete active space self-consistent field (CASSCF) method [57] in conjunction with the subsequent internally contracted multi-reference configuration interaction (icMRCI)

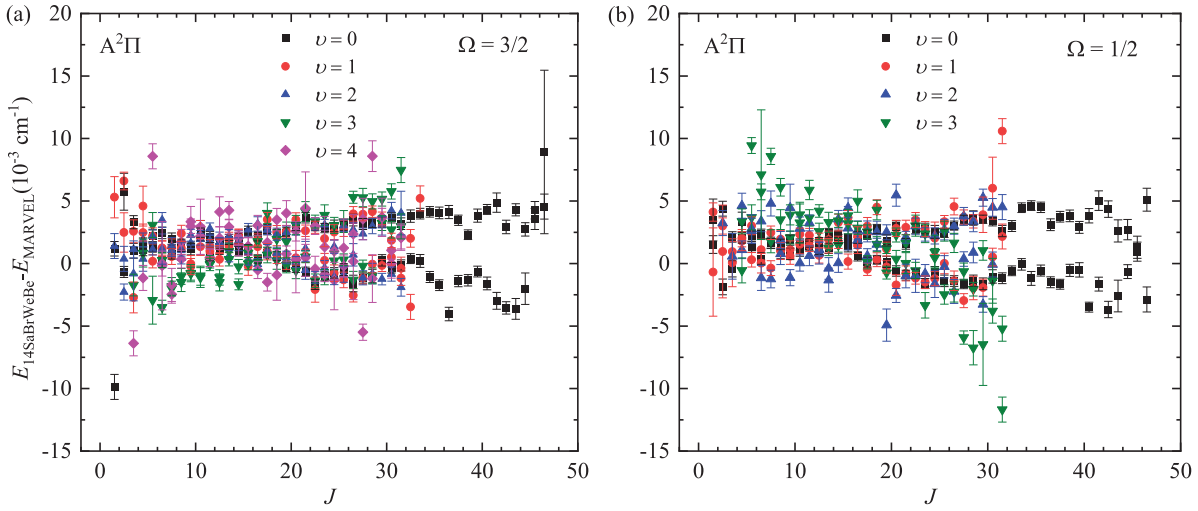

Fig. 2. Comparison of the empirical energy levels for the $A^2\Pi$ state from Ram et al. [35] with the MARVEL data. The residuals $E_{14RaBrWeBe}$-E_{MARVEL} for energy term values are plotted versus the rotational quantum number J for (a) the Ω=3/2 states and for (b) the Ω=1/2 states. The vertical bars represent the values of the uncertainty for MARVEL energy term values.

approach [58,59] with the Davidson correction (+Q), as implemented in the MOLPRO 2015 software package [60]. The core-valence correlation and scalar relativistic correlation corrections are also considered. The methodology and parameter settings are described in detail by Qin et al. [36]. These two PECs are directly taken from the publication of Qin et al. [36].

Except for *ab initio* PECs, *ab initio* EAMCs and SOCCs are also needed so as to obtain reliable analytical curves. Hence, they are calculated at the icMRCI/aug-cc-pV6Z [61,62] level of theory in this work. Nine valence electrons of CP are put into nine outermost molecular orbitals (i.e., 5–9σ, 2π and 3π), which constitute the active space, denoted as (5, 2, 2, 0). The remaining twelve inner electrons are put into six closed-shell molecular orbitals (i.e., 1–4σ and 1π). There are no available EAMCs for the $X^2\Sigma^+$ and $A^2\Pi$ electronic states in previous publications. Our calculated SOCCs of the $X^2\Sigma^+$ and $A^2\Pi$ electronic states are in good agreement with those computed by Abbiche et al. [34], just as shown in Fig. 4.

3.2. Refinements and spectroscopic models

The energy levels calculated directly by *ab initio* curves are not sufficiently useful for high-precision studies, so the empirical curves are needed by fitting to the experimental energy terms in order to generate rovibrational energy term values of sufficient accuracy. In this work, empirical PECs of both the $X^2\Sigma^+$ and $A^2\Pi$ electronic states were represented by an Extended Morse Oscillator (EMO) function [63] given by

$$V(r) = V_e + (A_e - V_e)[1 - \exp(-\beta_{EMO}(r)(r - r_e))]^2, \quad (1)$$

where V_e is the electronic excitation energy, A_e–V_e =D_e is the dissociation energy, A_e is the corresponding dissociation limit, r_e is the equilibrium internuclear distance of a PEC, and β_{EMO} is the distance-dependent exponent coefficient, defined as

$$\beta_{EMO}(r) = \sum_{k=0}^{N} B_k \xi_p^k \quad (2)$$

where N is the expansion order parameter, and ξ_p is the Šurkus variable [64] as shown by

$$\xi_p = \frac{r^p - r_e^p}{r^p + r_e^p}. \quad (3)$$

where p is an adjustable parameter for accurately fitting the PECs.

Table 1
Fitting parameters of empirical EMO potentials of the $X^2\Sigma^+$ and $A^2\Pi$ electronic states for CP.

Parameters	PEC ($X^2\Sigma^+$)	PEC ($A^2\Pi$)
V_e (cm^{-1})	0	6972.4689353
r_e (Å)	1.56197682784457	1.654417215765
D_e (cm^{-1})	43,203.88	4332.143893
p	6	3
N_L	1	1
N_R	8	6
B_0	2.13700409540576	1.99655694242876
B_1	0.246860442888354	0.042821211915037
B_2	−0.125091344945808	0.954400158866344
B_3	1.03509803608244	−0.124260985122129
B_4	−1.23975406930651	
B_5	−1.86671297523699	
B_6	4.29808754319990	
B_7	−0.0456673713783056	

Here, the MARVEL energy term values were used to fit the empirical PECs. The V_e values were set to 0 and 6972.46892 cm^{-1} for the $X^2\Sigma^+$ and $A^2\Pi$ electronic states, respectively, which are given by Ram et al. [35]. The dissociation energy of the $X^2\Sigma^+$ electronic state $D_e^{(X)}$ was fixed to 5.3566 eV obtained by the experimental $D_0^{(X)}$ = 5.28 eV [65] with an *ab initio* vibrational energy correction from Shi et al. [33]. The asymptote limit of the $A^2\Pi$ electronic state was estimated as $D_e^{(X)}$ − $V(A)$ e = 4.492 eV with the electronic excitation energy $V(A)$ e of the $A^2\Pi$ electronic state taken from Ram et al. [35]. The final set of fitting parameters is presented in Table 1.

For the SOCCs and EAMCs, we did not refine them analytically. Instead, the morphing procedure [66,67] was used for their refinement, as implemented in DUO. Thus, *ab initio* SOCCs and EAMCs were morphed by scaling them by a function $F(r)$ represented by

$$F(r) = \sum_{k=0}^{N} B_k z^k (1 - \xi_p) + \xi_p B_\infty, \quad (4)$$

where z is taken as a damped-coordinate polynomial, shown as follows

$$z = (r - r_{ref}) e^{-\beta_2 (r - r_{ref})^2 - \beta_4 (r - r_{ref})^4}. \quad (5)$$

where r_{ref} is a reference position equal to the equilibrium internuclear distance r_e by default, β_2 and β_4 are adjustable factors, the

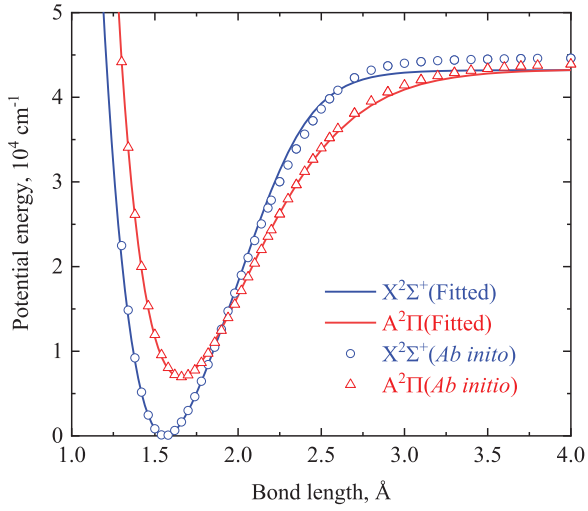

Fig. 3. Fitted EMO potentials and calculated *ab initio* potentials of the $X^2\Sigma^+$ and $A^2\Pi$ states for CP. The EMO potentials (solid line) is obtained by fitting the MARVEL energy levels obtained in Section 2. *Ab initio* potentials of the $X^2\Sigma^+$ state (circles) and the $A^2\Pi$ state (triangles) are taken from Qin et al. [36].

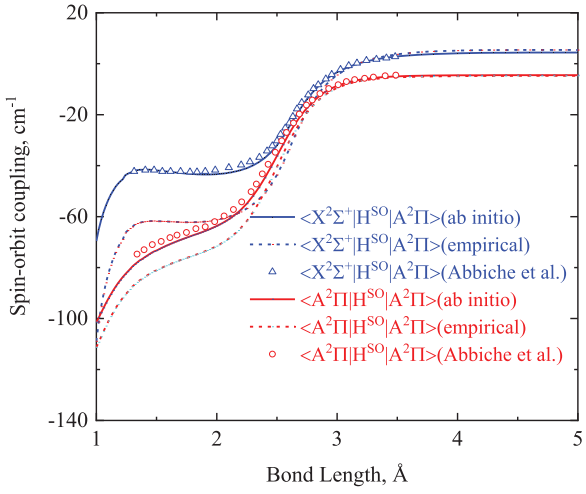

Fig. 4. Off-diagonal < $X^2\Sigma^+$|H^{SO}| $A^2\Pi$> (blue) and diagonal < $A^2\Pi$|H^{SO}| $A^2\Pi$> (red) SOCCs of CP. *Ab initio* values (solid line) are calculated by the icMRCI/aug-cc-pV6Z method and compared well with those (circles and triangles) calculated by Abbiche et al. [34] at the MRCI/aug-cc-pVQZ level of theory. Empirical curves (dash line) are obtained by morphing *ab initio* values as implemented in DUO.

parameter B_∞ is the value of the morphing function as $r \to \infty$ and is usually fixed at 1.

To account for rotational Born-Oppenheimer breakdown (BOB) effects [68] which become more and more important as J get larger, the vibrational energy operator was extended by

$$-\frac{\hbar^2}{2\mu r^2} \to -\frac{\hbar^2}{2\mu r^2}\left(1+g^{BOB}(r)\right), \tag{6}$$

where $\hbar$ is the reduced Planck constant, μ is the reduced mass, and g^{BOB} (r) is referred to as BOB curves, also represented by $F(r)$ function [Eqs. (4) and (5)]. Similar treatments were also applied to SRCs.

The Λ-doubling effects in DUO can be modelled using an effective Λ-doubling function. The Λ-doubling coupling for the $A^2\Pi$ electronic state was considered here using the following function [69]

$$\hat{H}_{LD}=\frac{1}{2}\alpha^{LD}_{opq}(r)\left(\hat{S}^2_+ + \hat{S}^2_-\right)-\frac{1}{2}\alpha^{LD}_{p2q}(r)\left(\hat{J}_+\hat{S}_+ + \hat{J}_-\hat{S}_-\right) \tag{7}$$

where $\alpha^{LD}_{opq}(r)$ and $\alpha^{LD}_{p2q}(r)$ are described by F(r) function.

Finally, the fitted parameters for all the curves represented our analytical spectroscopic models for CP can be found in the DUO input file provided as the supplemental material. The PECs, SOCCs and other coupling curves are shown in Figs. 3-8.

3.3. Accuracy of fits

The fitted analytical functions in Section 3.2 are included in the DUO program to calculate the rovibrational energy levels of the $X^2\Sigma^+$ and $A^2\Pi$ states (denoted as E_{fit}). Fig. 9 presents an overview of the $E_{\mathrm{MARVEL}}-E_{\mathrm{fit}}$ values. As shown in Fig. 9, the analytical spectroscopic models can reproduce relatively good rovibrational energy term values of the $X^2\Sigma^+$ state. The energy levels of the $A^2\Pi$ state are fitted with the errors below 0.1 cm^{-1}. Fig. 10 displays the E_{MARVEL}-$E_{\mathrm{Ab\ initio}}$ residuals for the $X^2\Sigma^+$ and $A^2\Pi$ states as a function of the J quantum number. Comparing with the results in Fig 9 and Fig 10, the fitted rovibrational energy levels are more accurate than *ab initio* ones. Hence, the fitted rovibrational energy levels for the $X^2\Sigma^+$ and $A^2\Pi$ states with a maximum vibrational quantum number of 59 and a maximum rotational quantum number of 200.5 are given in the supplemental material for potential applications.

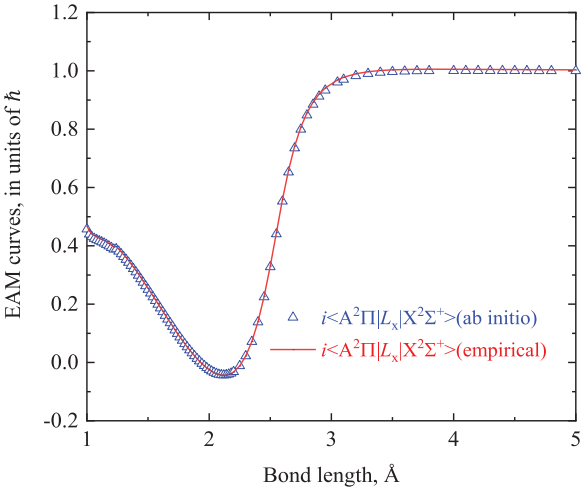

Fig. 5. The empirical EAMC (solid line) morphed by *ab initio* values (triangles) between the $X^2\Sigma^+$ and $A^2\Pi$ electronic states of CP.

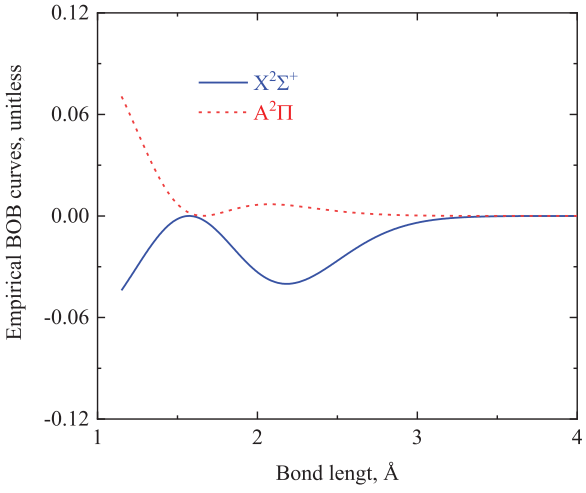

Fig. 6. Empirical BOBCs for the $X^2\Sigma^+$ and $A^2\Pi$ electronic states of CP.

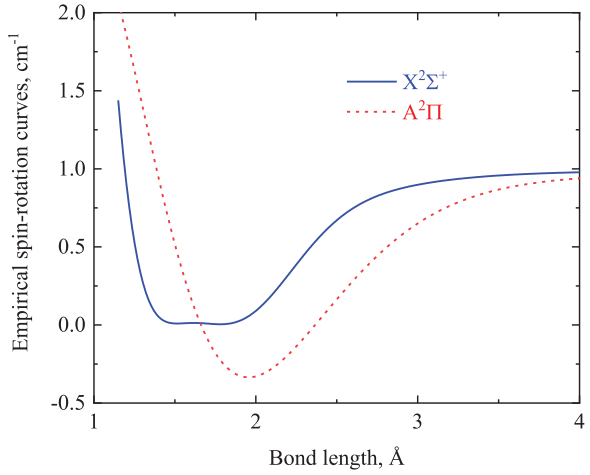

Fig. 7. Empirical SRCs for the $X^2\Sigma^+$ and $A^2\Pi$ electronic states of CP.

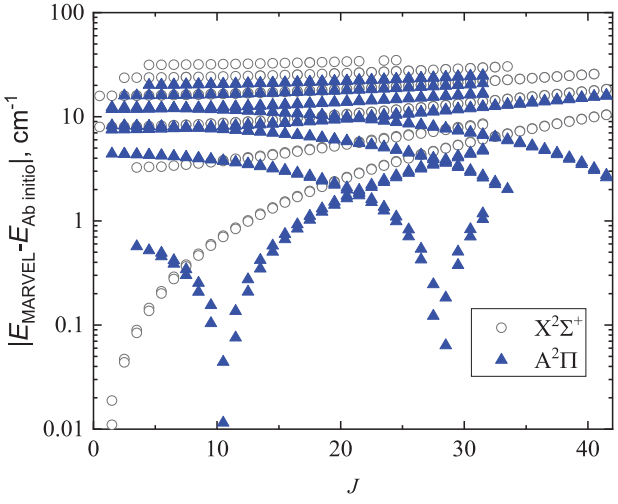

Fig. 10. The E_{MARVEL}-$E_{Ab\ initio}$ residuals for the $X^2\Sigma^+$ and $A^2\Pi$ states as a function of the J quantum number. The $X^2\Sigma^+$ and $A^2\Pi$ states both covers the vibrational levels up to υ =4 with the energy range from 0 to 12,000 cm^{-1}.

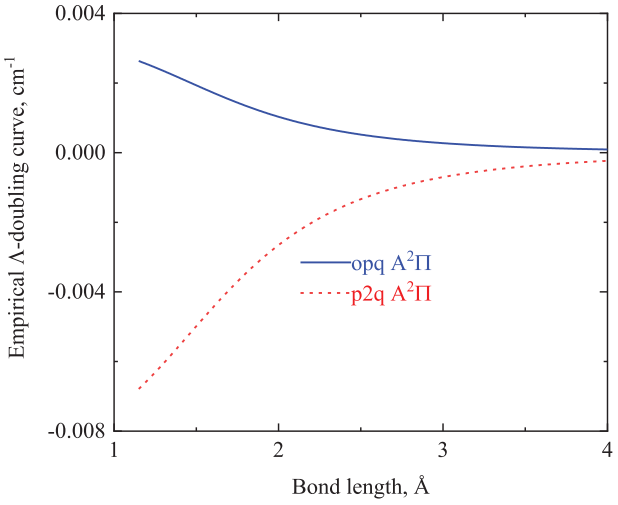

Fig. 8. Empirical Λ-doubling curves used for the $A^2\Pi$ electronic state of CP.

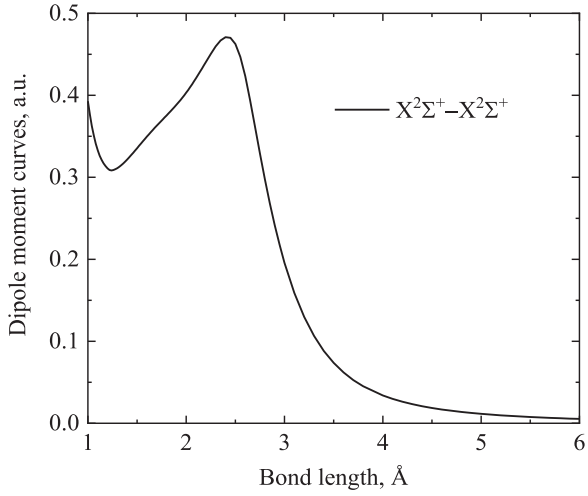

Fig. 11. *Ab initio* dipole moments of the $X^2\Sigma^+$ electronic state for CP.

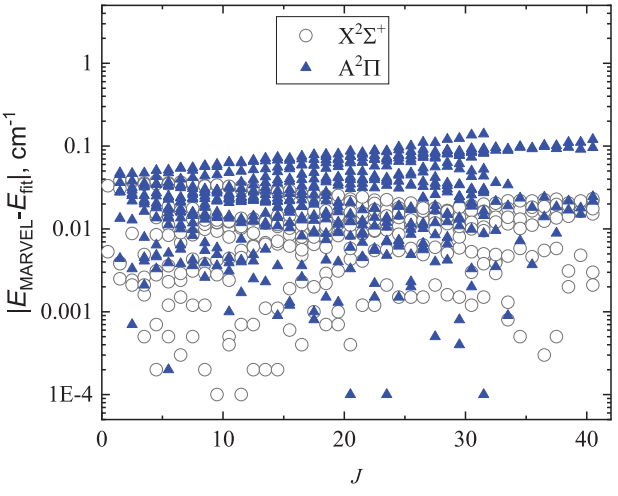

Fig. 9. The $E_{MARVEL}-E_{fit}$ residuals for the $X^2\Sigma^+$ and $A^2\Pi$ states as a function of the J quantum number. The $X^2\Sigma^+$ and $A^2\Pi$ states both covers the vibrational levels up to υ =4 with the energy range from 0 to 12,000 cm^{-1}.

3.4. Line lists for the $X^2\Sigma^+$- $X^2\Sigma^+$, $A^2\Pi$- $A^2\Pi$ and $A^2\Pi$- $X^2\Sigma^+$ transitions

The dipole moments (DMs) of the $X^2\Sigma^+$ state and $A^2\Pi$ state are computed by the icMRCI/aug-cc-pV6Z method and presented in Fig. 11 and Fig. 12, respectively. The TDMs for the $A^2\Pi$- $X^2\Sigma^+$ transition are selected from our previous publication [36]. Finally, the analytical spectroscopic models, *ab initio* DMs of the $X^2\Sigma^+$ state and $A^2\Pi$ state and *ab initio* TDMs for the $A^2\Pi$- $X^2\Sigma^+$ transition are included in DUO to compute the line lists for the $X^2\Sigma^+$- $X^2\Sigma^+$, $A^2\Pi$- $A^2\Pi$ and $A^2\Pi$- $X^2\Sigma^+$ transitions, which are provided in the supplemental material. DUO is a general program developed by Yurchenko et al. [51] for calculating the line lists of diatomic molecules described by various coupling curves. The theory is detailed in a published paper [52]. Technically, the vibrational basis set is established by solving two uncoupled Schrödinger equations using the sinc discrete variable representation (DVR) method. Rotational and spin basis set functions are constructed by the spherical harmonics $|J, \Omega\rangle$ and $|S, \Sigma\rangle$, respectively. DUO calculates Einstein *A*

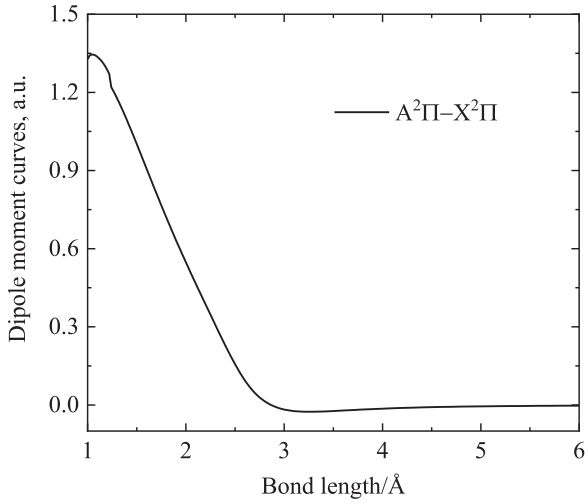

Fig. 12. *Ab initio* dipole moments of the $A^2\Pi$ electronic state for CP.

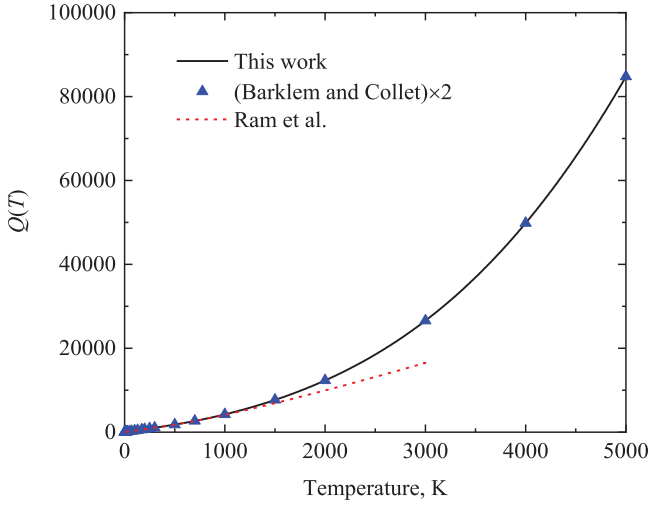

Fig. 13. Comparison of the temperature-dependent partition function of CP computed by our energy levels with that of Barklem & Collet [70] and Ram et al. [35].

coefficients in s^{-1} for a transition $\lambda_f \leftarrow \lambda_i$ by [51]

$$A_{fi} = \frac{64\times10^{-36}\pi^4}{3h}(2J_i+1)\nu^3 \times \sum_{t=-1,0,1}\left|\sum_{n_i,n_f}\left(C^{J_i,\tau_i}_{\lambda_i,n_f}\right)^* C^{J_i,\tau_i}_{\lambda_i,n_i}(-1)^{\Omega_i}\begin{pmatrix} J_i & 1 & J_f \\ \Omega_i & t & -\Omega_f\end{pmatrix}\langle\upsilon_f|\tilde{\mu}_t^{-f,i}(r)|\upsilon_i\rangle\right|^2 \quad (8)$$

where ν is the frequency, $\tilde{\mu}_t$ is the electronically averaged body-fixed component of the electric dipole moment (in Debye). The meaning of other parameters can refer to the paper of Yurchenko et al. [51].

4. Partition function

The partition function $Q(T)$ of CP was calculated with EXOCROSS [55] by explicit summation of the computed energy levels. $Q(T)$ is defined as [55]

$$Q(T) = \sum_n g_n^{ns}(2J_n+1)e^{c_2\tilde{E}_n/T} \quad (9)$$

where g_n^{ns} is the nuclear-spin statistical factor, c_2 $(=hc/k_B)$ is the second radiation constant (cm·K), $\tilde{E}_n(=E_n/hc)$ is the energy term value (cm^{-1}), and T is the temperature (K).

The fitted rovibrational energy levels of the $X^2\Sigma^+$ and $A^2\Pi$ electronic states both covering a maximum vibrational quantum number of 59 and a maximum rotational quantum number of 200.5 are used to calculate the partition function of CP for temperatures up to $T = 5000$ K in steps of 1 K. The partition function obtained here includes full atomic nuclear spin degeneracy. The nuclear spins of ^{12}C and ^{31}P considered here are 0 and 0.5, respectively, so the nuclear statistical weight is 2. For comparison, the partition function of Barklem & Collet [70] needs to be scaled by two times. Fig. 13 shows the temperature-dependent partition function of CP compared with those calculated by Barklem & Collet [70] and Ram et al. [35]. Our result agrees very well with that calculated by Barklem & Collet [70] up to 5000 K. Both results are larger than that of Ram et al. [35] for $T > 1000$ K. This is because Ram et al. considered the energy levels for $\upsilon = 0$–4, $J = 0.5$–65.5 and $\upsilon = 5$–8, $J = 0.5$–30.5. As a check, the partition function for $\upsilon = 0$–4, $J = 0.5$–65.5 and $\upsilon = 5$–8, $J = 0.5$–30.5 was calculated using our energy levels for comparison with that of Ram et al. [35]. Good agreement is observed. Therefore, the difference between our partition function (or that of Barklem & Collet) and that of Ram et al. is due mainly to the different amounts of energy levels considered.

Table 2
Polynomial coefficients fitted by Eq. (12) to represent the partition function of CP. The fit coefficients are valid for temperatures up to 5000 K.

Polynomial coefficient	CP
a_0	0.71037
a_1	0.80736
a_2	−0.18267
a_3	0.40078
a_4	−0.23225
a_5	0.05371
a_6	−0.00401

For ease of use, the polynomial fit of the partition function of CP was carried out by using the following function that was employed by Vidler & Tennyson [71]:

$$\log_{10}Q = \sum_{n=0}^{n_{max}} a_n(\log_{10}T)^n \quad (10)$$

where the polynomial coefficients a_n $(n = 0$–$6)$ are provided in Table 2. The fitted coefficients are valid for temperatures up to 5000 K.

5. Simulated spectra

In the following, we present different spectra of CP calculated using our line lists and utilizing the program EXOCROSS [55]. Fig. 14 gives an overview of the $X^2\Sigma^+$-$X^2\Sigma^+$ line list of CP in the form of absorption cross sections for a range of temperatures from 300 to 2000 K. Similar absorption cross sections exhibit in Fig. 15 and Fig. 16 for the $A^2\Pi$-$A^2\Pi$ transition and the $A^2\Pi$-$X^2\Sigma^+$ transition, respectively. At 2000 K, the contribution of the $A^2\Pi$-$X^2\Sigma^+$, $X^2\Sigma^+$- $X^2\Sigma^+$and $A^2\Pi$-$A^2\Pi$ bands to the simulated spectra is shown in Fig. 17.

Comparisons with the previous experimental work have been made to assess the quality of our line lists. Fig. 18 compares a portion of the spectrum of the 0–0 band for the $A^2\Pi_{3/2}$-$X^2\Sigma^+$ spectrum of CP observed by Ram et al. [35] with that computed using our line lists assuming a temperature of 2000 K (vibrational) and 720 K (rotational), showing good agreement. Fig 19 shows a comparison between the 1–0 band of the $A^2\Pi_{1/2}$-$X^2\Sigma^+$ spectrum of CP

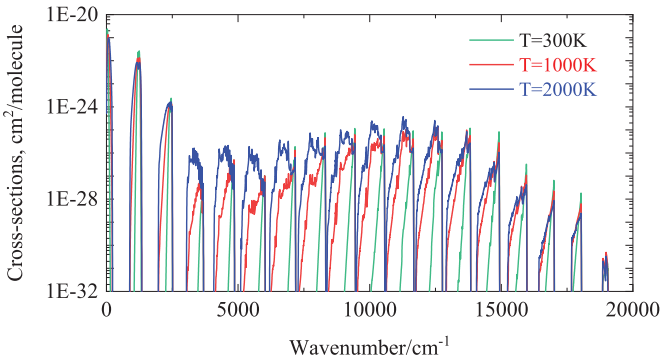

Fig. 14. Temperature dependence of CP cross-sections obtained by using the line list of the $X^2\Sigma^+$-$X^2\Sigma^+$ transition and a Gaussian profile with a Half Width at Half Maximum (HWHM) = 5 cm^{-1}, from bottom to top: T = 300, 1000 and 2000 K.

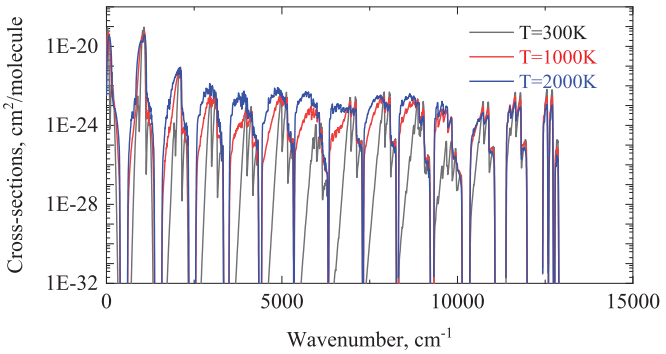

Fig. 15. Temperature dependence of CP cross-sections obtained by using the line list of the $A^2\Pi$-$A^2\Pi$ transition and a Gaussian profile with a HWHM = 5 cm^{-1}, from bottom to top: T = 300, 1000 and 2000 K.

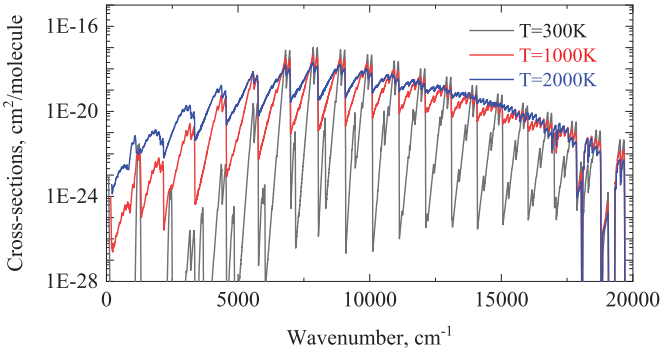

Fig. 16. Temperature dependence of CP cross-sections obtained by using the line list of the $A^2\Pi$-$X^2\Sigma^+$ transition and a Gaussian profile with a HWHM = 5 cm^{-1}, from bottom to top: T = 300, 1000 and 2000 K.

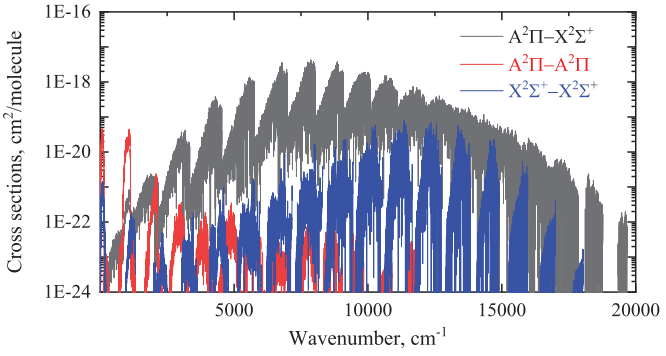

Fig. 17. Contribution of each band (the $A^2\Pi$-$X^2\Sigma^+$, $X^2\Sigma^+$- $X^2\Sigma^+$and $A^2\Pi$-$A^2\Pi$ bands) to the simulated spectra of CP at 2000 K. A Gaussian profile with a HWHM = 0.05 cm^{-1} is used.

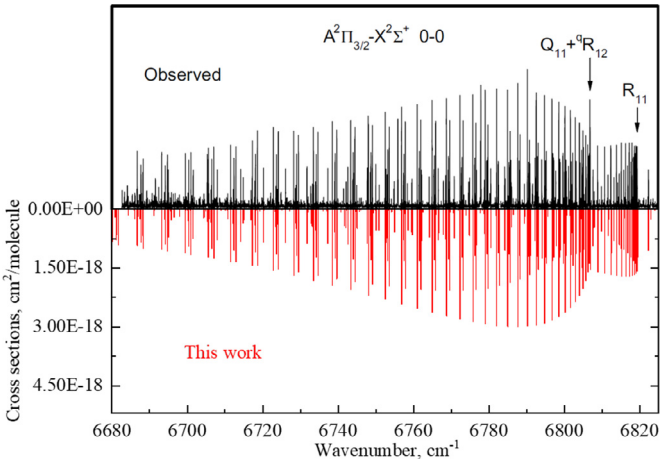

Fig. 18. Comparison between the 0–0 band of the $A^2\Pi_{3/2}$-$X^2\Sigma^+$ spectrum of CP observed by Ram et al. [35] (upper) and computed using our line lists (lower) assuming a temperature of 2000 K (vibrational) and 720 K (rotational).

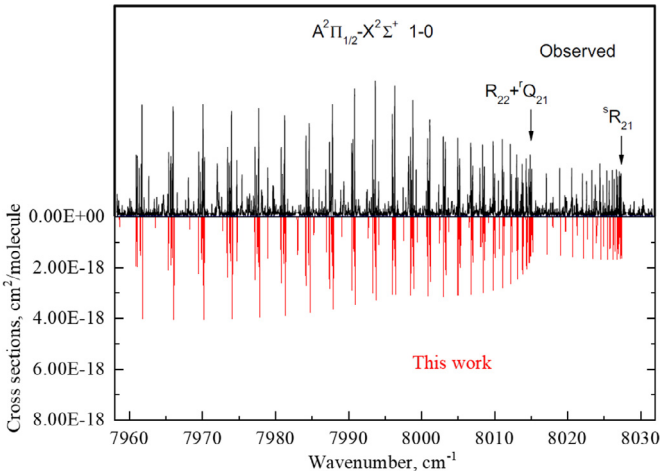

Fig. 19. Comparison between the 1–0 band of the $A^2\Pi_{1/2}$-$X^2\Sigma^+$ spectrum of CP observed by Ram et al. [35] (upper) and computed using our line lists (lower) assuming a temperature of 2000 K (vibrational) and 720 K (rotational).

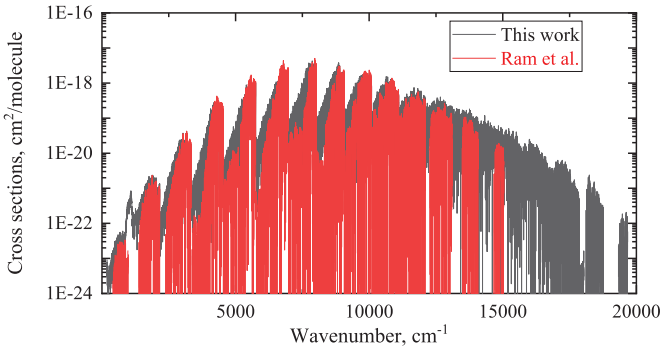

Fig. 20. Comparison between the cross sections calculated by our line lists of $A^2\Pi$-$X^2\Sigma^+$ transition and those computed by the line lists from Ram et al. [35].

observed by Ram et al. [35] and that computed using our line lists assuming a temperature of 2000 K (vibrational) and 720 K (rotational). As can be seen, a good correspondence exists as well. In addition, a comparison of our line list with that computed by Ram et al. [35] is displayed in Fig. 20. Below 11,000 cm^{-1}, the two line lists agree well. Above this, there are difference due to the inclusion of higher rovibronic transitions.

6. Conclusions

In this work, a set of 353 empirical rovibrational energy levels of the $X^2\Sigma^+$ state and 595 empirical rovibrational energy levels of the $A^2\Pi$ state for CP is generated by the MARVEL method for υ up to 4 and with rotational coverage up to a maximum $J = 46.5$, denoted as MARVEL energy levels. Good agreement with those of Ram et al. [35] can be observed within the uncertainty of 5.0×10^{-3} cm^{-1} for most of the rovibrational energy levels. The obtained 948 MARVEL energy levels can be used for high precision studies in astrophysics and are provided as supplementary material.

The MARVEL energy levels are then used to fit EMO potential energy functions for the $X^2\Sigma^+$ and $A^2\Pi$ electronic states and various coupling curves, including SOCCs, EAMCs, Born-Oppenheimer breakdown curves, SRCs and Λ-doubling curves. The analytical spectroscopic models are included into DUO to calculate the fitted energy levels for the $X^2\Sigma^+$ and $A^2\Pi$ states, which both cover a maximum vibrational quantum number of 59 and a maximum rotational quantum number of 200.5 and are provided as supplemental material. Subsequently, the analytical spectroscopic models are then used to compute the rovibrational line lists for the $A^2\Pi$-$X^2\Sigma^+$, $X^2\Sigma^+$- $X^2\Sigma^+$and $A^2\Pi$-$A^2\Pi$ transitions. These line lists are expected to be applied to spectroscopic detection of CP in astrophysics and to other potential applications.

The fitted energy levels for the $X^2\Sigma^+$ and $A^2\Pi$ electronic states are used to compute the values of partition function for temperatures up to $T = 5000$ K in steps of 1 K, which are presented as supplemental material. For ease of use, the temperature-dependent partition function is fitted by the polynomial expansion. Finally, the simulated spectra using our line lists compare with available experimental ones, showing good agreement.

The line lists in this work are given in the ExoMol format and provided in the supplemental material.

Declaration of Competing Interest

The authors declare that they have no known competing financial interests or personal relationships that could have appeared to influence the work reported in this paper.

CRediT authorship contribution statement

Zhi Qin: Investigation, Conceptualization, Methodology, Data curation, Writing - original draft, Writing - review & editing. **Tianrui Bai:** Software, Validation. **Linhua Liu:** Supervision, Funding acquisition, Conceptualization, Data curation, Writing - review & editing.

Acknowledgement

We acknowledge the support from the National Natural Science Foundation of China under Grant NO. 51421063. Zhi Qin acknowledge the programs of DUO and EXOCROSS developed and provided by ExoMol group at University College London. The referees are greatly appreciated for incisive comments, which led to considerable strengthening of this paper.

Supplementary materials

Supplementary material associated with this article can be found, in the online version, at doi:10.1016/j.jqsrt.2020.107352.

References

[1] Turner BE, Bally J. Detection of interstellar PN: the first identified phosphorus compound in the interstellar medium. Astrophys J. 1987;321(1):L75–9.
[2] Ziurys LM. Detection of interstellar PN: the first phosphorus-bearing species observed in molecular clouds. Astrophys. J. 1987;321(1–2):L81.
[3] Tenenbaum ED, Woolf NJ, Ziurys LM. Identification of Phosphorus Monoxide (X2Πr) in VY Canis Majoris: detection of the First PO Bond in Space. Apj 2007;666(1):L29–32.
[4] Milam SN, Halfen DT, Tenenbaum ED, Apponi AJ, Woolf NJ, Ziurys LM. Constraining phosphorus chemistry in carbon- and oxygen-rich circumstellar envelopes: observations of PN, HCP, and CP. Apj 2008;684(1):618–625.
[5] Yamaguchi T, Takano S, Sakai N, Sakai T, Liu S-Y, Su Y-N, Hirano N, Takakuwa S, Aikawa Y, Nomura H. Detection of phosphorus nitride in the lynds 1157 B1 shocked region. Publ. Astron. Soc. Jpn. 2011;63(5):L37–41.
[6] Beck ED, Kamiński T, Patel NA, Young KH, Gottlieb CA, Menten KM, Decin L. PO and PN in the wind of the oxygen-rich AGB star IK Tau. Astron. Astrophys. 2013;558(8):132–40.
[7] Fontani F, Rivilla VM, Caselli P, Vasyunin A, Palau A. Phosphorus-bearing molecules in massive dense cores. Astrophys. J. 2016;822(2):L30.
[8] Lefloch B, Vastel C, Viti S, Jimenezserra I, Codella C, Podio L, Ceccarelli C, Mendoza E, Lepine JRD, Bachiller R. Phosphorus-bearing molecules in solar-type star-forming regions: first PO detection. Mon. Not. Roy. Astron. Soc. 2016;462(4):3937–44.
[9] Rivilla VM, Fontani F, Beltrán MT, Vasyunin A, Caselli P, MartínPintado J, Cesaroni R. The first detections of the key prebiotic molecule PO in star-forming regions. Apj 2016;826(2):161.
[10] Mininni C, Fontani F, Rivilla VM, Beltrán MT, Caselli P, Vasyunin A. On the origin of phosphorus nitride in star-forming regions. Mon. Not. Roy. Astron. Soc. 2018;476:L39–44.
[11] Rivilla VM, Jiménezserra I, Zeng S, Martín S, Martínpintado J, Armijosabendaño J, Viti S, Aladro R, Riquelme D, Requenatorres M. Phosphorus-bearing molecules in the Galactic Center. Mon. Not. Roy. Astron. Soc. 2018;475:L30–4.
[12] Ziurys LM, Schmidt DR, Bernal JJ. New circumstellar sources of PO and PN: the increasing role of phosphorus chemistry in oxygen-rich stars. Astrophys. J. 2018;856(2):169.
[13] Jiménez-Serra I, Viti S, Quénard D, Holdship J. The Chemistry of Phosphorus-bearing Molecules under Energetic Phenomena. Astrophys. J. 2018;862(2):128.
[14] Bergner JB, Öberg KI, Walker S, Guzmán VV, Rice TS, Bergin EA. Detection of Phosphorus-bearing Molecules toward a Solar-type Protostar. Astrophys. J. Lett. 2019;884(2):L36.
[15] Fontani F, Rivilla V, van der Tak F, Mininni C, Beltrán M, Caselli P. Origin of the PN molecule in star-forming regions: the enlarged sample. Mon. Not. Roy. Astron. Soc. 2019;489(4):4530–42.
[16] Guelin M, Cernicharo J, Paubert G, Turner BE. Free CP in IRC+10216. Astron. Astrophys. 1990;230(1):L9–L11.
[17] Yu H-t, Zhao Y-l, Kan W, Fu H-g. A theoretical study on the radical–neutral reaction mechanism of carbon monophosphide, CP, with acetylene, C2H2. Theochem-J. Mol. Struct. 2006;772(1–3):45–50.
[18] Herzberg G. A new band system probably due to a molecule CP. Natur 1930;126(3169):131–2.
[19] Bärwald H, Herzberg G, Herzberg L. Bandenspektrum und struktur des CP–Moleküls. Ann. Phys. 1934;412(6):569–93.
[20] Chaudhry AK, Upadhya KN. 3Σ+-3Π band system in CP molecule. Indian. J. Phys. 1969:4383–91.
[21] Wentink T, Spindler RJ. Franck-Condon factors and r-centroids for NO+, CP, SiF, BF, BCl and BBr. J. Quant. Spectrosc. Radiat. Transf. 1970;10(6):609–19.
[22] N.S. Murthy, L.S. Gowda, B. Narasimhamurthy, Carbon phosphide (B2Σ+-A2Πi) band system: RKR Franck-Condon factors and r-centroids. PramanaPramana1976; 6(1): 25–28.
[23] Tripathi R, Rai SB, Upadhya KN. The B-A system of CP molecule. Pramana Pramana 1981;17(3):249–55.
[24] Ram RS, Bernath PF. Fourier transform spectroscopy of the A2Πi-X2Σ+ system of CP. J. Mol. Spectrosc. 1987;122(2):282–92.
[25] Rohlfing MM, Almlöf J. Theoretical determination of the dipole moment of carbon monophosphide, CP(X2Σ+). Chem. Phys. Lett. 1988;147(2):258–262.
[26] Saito S, Yamamoto S, Kawaguchi K, Ohishi M, Suzuki H, Ishikawa SI, Kaifu N. The microwave spectrum of the CP radical and related astronomical search. Astrophys. J. 1989;341(2):1114–19.
[27] Ram RS, Tam S, Bernath PF. The A2Πi-X2Σ+ system of CP: observation of new bands. J. Mol. Spectrosc. 1992;152(1):89–100.
[28] Reddy RR, Rao TVR, Viswanath R. Potential energy curves and dissociation energies of NbO, SiC, CP, PH+, SiF+, and NH+. Astrophys. Space Sci. 1992;189(1):29–38.
[29] Gu JP, Buenker RJ, Hirsch G. Ab initio CI study of the electronic spectrum of the interstellar free radical CP. Chem. Phys. 1994;185(1):39–45.
[30] de Brouckère G, Feller D. Configuration-interaction calculations of miscellaneous properties of the CP and CP- molecules: I. CP ground state. J. Phys. B-At. Mol. Opt. Phys. 1996;276(29):5283.
[31] de Brouckère G, Feller D. Configuration interaction calculations on the A2Πi state of CP and the A2Πi-X2Σ+ transition bands. Miscellaneous properties. J. Phys. B-At. Mol. Opt. Phys. 1998;31(23):513–38.
[32] Pascoli G, Lavendy H. Theoretical Study of CnP, CnP+, CnP− (n=1-7) Clusters. J. Phys. Chem. A, 103; 1999.
[33] Shi DH, Xing W, Sun JF, Zhu ZL, Liu YF. Extensive ab initio study of the electronic states of CP radical including spin-orbit coupling. Mol. Phys. 2012;276-277(5):1–9.

[34] Abbiche K, Marakchi K, Komiha N, Francisco JS, Linguerri R, Hochlaf M. Accurate theoretical spectroscopy of the lowest electronic states of CP radical. Mol. Phys. 2014;112(20):2633–45.
[35] Ram RS, Brooke JSA, Western CM, Bernath PF. Einstein A-values and oscillator strengths of the A2Π–X2Σ+ system of CP. J. Quant. Spectrosc. Radiat. Transf. 2014:138107–15.
[36] Qin Z, Zhao J, Liu L. Theoretical study on low-lying electronic states of CP radical: energy levels, Einstein coefficients, Franck-Condon factors and radiative lifetimes. J. Quant. Spectrosc. Radiat. Transf. 2019:23036–47.
[37] Endres CP, Schlemmer S, Schilke P, Stutzki J, Müller HS. The cologne database for molecular spectroscopy, CDMS, in the virtual atomic and molecular data centre, VAMDC. J. Mol. Spectrosc. 2016 32795-104.
[38] Császár AG, Czakó G, Furtenbacher T, Mátyus E. An active database approach to complete rotational–vibrational spectra of small molecules. Annu Rep Comput Chem 2007:3155–76.
[39] Furtenbacher T, Császár AG, Tennyson J. MARVEL: measured active rotational–vibrational energy levels. J. Mol. Spectrosc. 2007;245(2):115–25.
[40] Furtenbacher T, Csaszar AG. MARVEL: measured active rotational–vibrational energy levels. II. Algorithmic improvements. J. Quant. Spectrosc. Radiat. Transf. 2012;113(11):929–35.
[41] Tóbiás R, Furtenbacher T, Tennyson J, Császár AG. Accurate empirical rovibrational energies and transitions of H216O. Phys. Chem. Chem. Phys. 2019;21(7):3473–95.
[42] Császár AG, Furtenbacher T, networks Spectroscopic. J. Mol. Spectrosc. 2011;266(2):99–103.
[43] Furtenbacher T, Császár AG. The role of intensities in determining characteristics of spectroscopic networks. J. Mol. Struct. 2012:1009123–9.
[44] Furtenbacher T, Arendás P, Mellau G, Császár AG. Simple molecules as complex systems. Scientific Reports 2014:44654.
[45] Árendás P, Furtenbacher T, Császár AG. On spectra of spectra. J. Math. Chem. 2016;54(3):806–22.
[46] McKemmish LK, Masseron T, Sheppard S, Sandeman E, Schofield Z, Furtenbacher T, Csaszar AG, Tennyson J, Sousa-Silva C. MARVEL analysis of the measured high-resolution rovibronic spectra of 48Ti16O. Astrophys. J. Suppl. Ser. 2017:22815.
[47] McKemmish LK, Borsovszky J, Goodhew KL, Sheppard S, Bennett AF, Martin AD, Singh A, Sturgeon CA, Furtenbacher T, Császár AG. Marvel Analysis of the Measured High-resolution Rovibronic Spectra of 90Zr16O. Astrophys. J. 2018;867(1):33.
[48] Furtenbacher T, Horváth M, Koller D, Sólyom P, Balogh A, Balogh I, Császár AG. MARVEL analysis of the measured high-resolution rovibronic spectra and definitive ideal-gas thermochemistry of the 16O2 molecule. J. Phys. Chem. Ref. Data 2019;48(2):023101.
[49] Darby-Lewis D, Shah H, Joshi D, Khan F, Kauwo M, Sethi N, Bernath PF, Furtenbacher T, Tóbiás R, Császár AG. MARVEL analysis of the measured high-resolution spectra of 14NH. J. Math. Chem. 2019:36269–76.
[50] Tennyson J, Yurchenko SN. The ExoMol project: software for computing large molecular line lists. Int. J. Quantum Chem. 2017;117(2):92–103.
[51] Yurchenko SN, Lodi L, Tennyson J, Stolyarov AV. Duo: a general program for calculating spectra of diatomic molecules. Computer Physics Communications 2016:202262–75.
[52] Tennyson J, Lodi L, McKemmish LK, Yurchenko SN. The ab initio calculation of spectra of open shell diatomic molecules. J. Phys. B-At. Mol. Opt. Phys. 2016;49(10):102001.
[53] Li HY, Tennyson J, Yurchenko SN. ExoMol line lists – XXXII. The rovibronic spectrum of MgO. Mon. Not. Roy. Astron. Soc. 2019(2):2351–65.
[54] Yurchenko SN, Williams H, Leyland PC, Lodi L, Tennyson J. ExoMol linelists XXVIII: the rovibronic spectrum of AlH. Mon. Not. Roy. Astron. Soc. 2018:4791401–11.
[55] Yurchenko SN, Al-Refaie AF, Tennyson J. ExoCross: a general program for generating spectra from molecular line lists. Astron. Astrophys. 2018;614:A131.
[56] Prajapat L, Jagoda P, Lodi L, Gorman MN, Yurchenko SN, Tennyson J. ExoMol molecular line lists – XXIII. Spectra of PO and PS. Mon. Not. Roy. Astron. Soc. 2017;472(3):3648–58.
[57] Werner HJ, Knowles PJ. A second order multiconfiguration SCF procedure with optimum convergence. J Chem Phys 1985;82(11):5053–63.
[58] Knowles PJ, Werner HJ. An efficient method for the evaluation of coupling coefficients in configuration interaction calculations. Chem. Phys. Lett. 1988;145(6):514–22.
[59] Werner HJ, Knowles PJ. An efficient internally contracted multiconfiguration reference CI method. Journal of Chemical Physics 1988;89(9):5803–14.
[60] H.J. Werner, P.J. Knowles, G. Knizia, F.R. Manby, a. others, MOLPRO 2015, a package of ab initio programs, see http://www.molpro.net.
[61] Woon DE, Dunning TH. Gaussian basis sets for use in correlated molecular calculations. IV. Calculation of static electrical response properties. Journal of Chemical Physics 1993;98(2):1358–71.
[62] Woon DE, Dunning TH Jr.. Gaussian basis sets for use in correlated molecular calculations. V. Core-valence basis sets for boron through neon. Journal of Chemical Physics 1995;103(11):4572–85.
[63] Lee EG, Seto JY, Hirao T, Bernath PF, Le Roy RJ. FTIR emission spectra, molecular constants, and potential curve of ground state GeO. J. Mol. Spectrosc. 1999;194(2):197–202.
[64] Šurkus A, Rakauskas R, Bolotin A. The generalized potential energy function for diatomic molecules. Chem. Phys. Lett. 1984;105(3):291–4.
[65] Huber KP, Herzberg G. Molecular spectra and molecular structure, vol. IV: constants of diatomic molecules. New York: Van Nostrand Reinhold; 1979.
[66] Meuwly M, Hutson JM. Morphing ab initio potentials: a systematic study of Ne–HF. J. Chem. Phys. 1999;110(17):8338–47.
[67] Patrascu AT, Hill C, Tennyson J, Yurchenko SN. Study of the electronic and rovibronic structure of the X2Σ+, A2Π, and B2Σ+ states of AlO. J. Chem. Phys. 2014;141(14):144312.
[68] Le Roy RJ. LEVEL: a computer program for solving the radial Schrödinger equation for bound and quasibound levels. J. Quant. Spectrosc. Radiat. Transf. 2017:186167–78.
[69] Brown J, Merer A. Lambda-type doubling parameters for molecules in Π electronic states of triplet and higher multiplicity. J. Mol. Spectrosc. 1979;74(3):488–94.
[70] Barklem PS, Collet R. Partition functions and equilibrium constants for diatomic molecules and atoms of astrophysical interest. Astron. Astrophys. 2016;588:A96.
[71] Vidler M, Tennyson J. Accurate partition function and thermodynamic data for water. J. Chem. Phys. 2000;113(21):9766–71.